cyanide electrolyte will either oxidize cyanide to cyanate if such a process is electrochemically active, or act to photodecompose the CdSe. Cyanate, redundantly analyzed by both FTIR and ion exchange chromatography (17), is not detectable in solution during 6 h of 20 mA/cm^2 photodecomposition of n-CdSe in 1.0*M* KCN, 0.5*M* KOH, showing that electrochemical oxidation of cyanide is not significant in this PEC. Under illumination the process continues until the electrode is fully consumed and dissolved. CdSe mass loss correlates with buildup of solution cadmium, as determined by atomic absorption analysis of the electrolyte. We observe that cyanide dissolves the cadmium decomposition product forming $Cd(CN)_4^{2-}$. Thus, higher levels of solution cyanide may enhance photocurrent and effective quantum yield by favoring decomposition over alternative competing recombination.

We conclude that the reported battery effect (4) does not exist and that the electrolyte modification approach can yield stable PECs and unusually high photovoltages and solar to electrical conversion efficiencies.

Acknowledgments

S. Licht is grateful to the Carl Julius and Anna (Kranz) Carlson Chair in Chemistry for financial support of this work.

Manuscript submitted Sept. 9, 1991; revised manuscript received Dec. 6, 1991.

Clark University assisted in meeting the publication costs for this letter.

REFERENCES

1. B. A. Parkinson, *Accts. Chem. Res.*, **17,** 431 (1984).
2. S. Licht, **Nature, 330,** 148 (1987), and references therein.
3. (a) S. Licht and d. Peramunage, *ibid.*, **345,** 330 (1990); (b) *ibid.*, **354,** 440 (1991).
4. G. Seshardi, J. K. M. Chun, and A. B. Bocarsly, *ibid.*, **352,** 508 (1991).
5. G. H. Kelsall, *This Journal*, **138,** 108 (1991).
6. G. H. Kelsall, S. Savage, and D. Brandt, *ibid.*, **138,** 117 (1991).
7. H. Schmidt and H. Meinert, *Z. Anorg. u. allgem. chemie*, **293,** 214 (1957).
8. R. D. Rocklin and E. L. Johnson, *Anal. Chem.*, **55,** 4 (1983).
9. A. M. Bond, I. D. Heritage, G. G. Wallace, and M. J. McCormick, *ibid.*, **54,** 582 (1982).
10. D. T. Sawyer and R. J. Day, *J. Electroanal. Chem.*, **5,** 195 (1963).
11. A. S. Hinman, R. A. Kydd, and R. P. Cooney, *J. Chem. Soc. Faraday Trans. 1*, **82,** 3525 (1986).
12. A. W. Adamson, J. P. Welker, and M. Volpe, *J. Amer. Chem. Soc.*, **72,** 4030 (1950).
13. S. Asperger, I. Murati, and D. Pavlovic, *J. Chem. Soc. London*, 730 (1960).
14. Ph. Allongue and R. Tenne, *This Journal*, **138,** 261 (1991).
15. H. Gerischer and W. Mindt, *Electrochim. Acta.*, **13,** 1329 (1968).
16. V. Marcu and H.-H. Strehblow, *This Journal*, **138,** 108 (1991).
17. W. H. R. Shaw and J. J. Bordeaux, *Anal. Chem.*, **27,** 136 (1955).
18. G. Hodes, in "Energy Resources through Photochemistry and Catalysis," M. Gratze, Editor, Academic Press, New York (1983).

Buckling of Anodic Films. A Mechanism for the Breakdown of Coatings on Aluminum Wires

O. Teschke* and M. U. Kleinke

Instituto de Fisica, UNICAMP 13081, Campinas, SP, Brazil

ABSTRACT

Oxide layer mechanical instability on anodized aluminum is reported. The striated structure is formed by a regular arrangement of straight lines parallel to the rod axis. A special cell with an axially symmetric current distribution was constructed in order to generate an isotropic stress distribution. The patterns are only formed when the anodization charge density is larger than a critical value. Our results show that film stress values are a function of the anodizing current density.

Anodic films are subjected to mechanical stresses during their formation (1, 2). These stresses have been measured by clamping the upper end of a thin foil of the metal and observing the motion of the lower end (3, 4). The formula for calculating stress in terms of the end deflection assumes that Young's modulus of both the film and the substrate is identical and that the stress is isotropic. The theory used to derive the equations is limited in its applicability as discussed by Klokholm (5) and Hoffman (6). In this paper we propose a method for measuring the stresses in anodic films on aluminum wires by determining the critical value of the stress for buckling of these films.

A special cell with an axially symmetric current distribution was built in order to generate a radially isotropic stress distribution. The test cell is schematically shown in Fig. 1. The cell walls and cover are made of PTFE. The electrolytic cell was operated at atmospheric pressure. The working electrode was a 4 cm long and 0.46 cm diam aluminum rod. The length of surface exposed to solution is adjustable from 2 mm to 2 cm; the counterelectrode is a cylindrical platinum mesh creating a radial current distribution. The radial distance between the two concentric electrodes is 1.5 cm. The specimens were prepared from the same aluminum wire (commercial grade 99.2% pure, supplied by ALCAN). They were abraded with emery paper (grid 600), polished with diamond paste (through 0.5 μm), and annealed at 300°C for 2 h in a 10^{-1} Torr atmosphere. The surfaces of the specimens were immersed in a chromic-phosphoric acid solution (20 g/l H_2CrO_4, 35 ml/l H_3PO_4) for 5 min at 82°C, washed with distilled water, and anodized. Anodic oxide films were formed at various current densities in a 7.5% sulfuric acid solution thermostated at 23°C. The electrolytic solution was prepared with doubly distilled water and sulfuric acid (analytical grade). The galvanostat is a PAR Model 273A Gal-

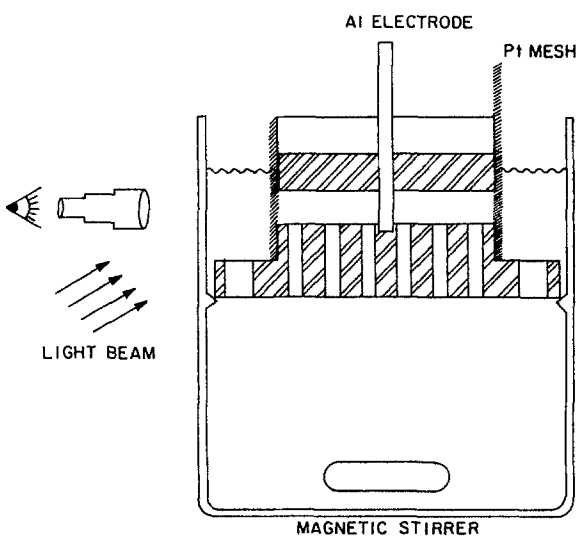

Fig. Schematic diagram of the test cell.

* Electrochemical Society Active Member.

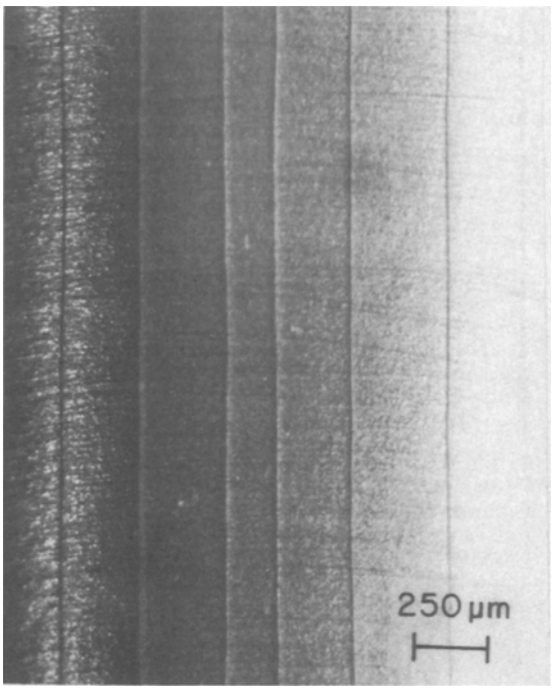

Fig. 2(a). Optical micrograph showing the buckling of the oxide film which resulted in an arrangement of a series of fringes along the outer periphery of the oxide film.

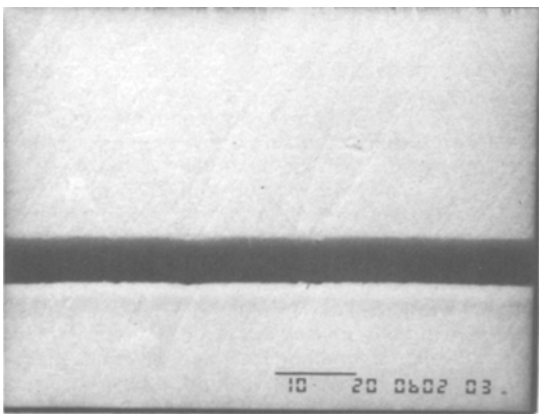

Fig. 2(b). SEM micrograph showing the crack formed at the striae cusps.

vanostat/Potentiostat. After their removal from the electrolyte, the electrodes were rinsed with distilled water, dried, introduced in a vacuum chamber and a gold layer of about 150 Å was evaporated over their surfaces. After the gold deposition, the electrode surfaces were examined in a JEOL TS-300 scanning electron microscope.

As the aluminum substrate is anodized, the compressive stress in the growing oxide film causes deformation. Figure 2 shows a series of fringes on an oxide film along the outer periphery of the aluminum rod. These fringes correspond to the maximum vertical displacement of the corrugated oxide film and they form a regular arrangement of straight lines parallel to the rod axis. The patterns are only formed when the anodization charge is larger than a critical value. When the electrode charge is smaller than this value the film surface remains smooth. For each current density the critical charge density is determined by the observation of the electrode surface by an

Table I. Anodic film stress data. The other parameters are the number of striae η, the estimated oxide film thickness $\bar{t}$ and the measured critical charge $\bar{Q}_c$.

I (mA/cm^2)	$\bar{Q}_c$ (C/cm^2)	$\bar{t}$ (μm)	η	Stress (Pa)
27	54.4	20.4	4	0.4×10^7
35	44.2	16.6	12	2.5×10^7
50	49.3	18.5	16	5.9×10^7
75	42.0	15.8	20	6.7×10^7
100	36.8	13.8	24	7.6×10^7
150	37.7	14.1	26	9.2×10^7
200	32.4	12.2	32	10.5×10^7

Olympus Model 52-TR-BR optical stereoscope. When the critical thickness of oxide is reached, the striae arrangement appears on the electrode surface and the process is stopped.

The buckling of the anodic film, which results in the regular arrangement of parallel lines to the rod axis, may be analyzed using a logic similar to that introduced by Euler to describe the mechanical instability of a cylinder under compressive forces. For a long cylinder of unit length uniformly compressed by external pressure, as long as the corresponding compressive stress does not exceed the fracture limit of the material, the critical value of the compressive stress, σ_c, is given by (7)

$$\sigma_c = \frac{h^2(n^2 - 1)}{12(1 - \nu^2)R^2} E$$

where E is the Young's modulus, ν is the Poisson's ratio, R is the radius, h is the wall thickness of the cylinder, and n is equal to number of striae.

For example, anodization of aluminum in a 7.5% aqueous sulfuric acid solution at 23°C, with a current density of 50 mA/cm^2 during 1000 s, generates a coating with 16 striae on the original smooth electrode surface. The calculated film stress for $E = 4.2 \times 10^{10}$ (4), obtained by the above expression is shown in Table I and is in agreement with the value obtained in Ref. (3) and (4).

Film buckling will take place if the compressive stress acting on the film exceeds the critical film stress value. If an efficient stress relieving mechanism is present for the film under appropriate anodization conditions, the film may never buckle as often occurs for low current densities (~10 mA/cm^2). The stress calculated from the deflection of foils is not a function of the oxide film thickness (4), while film stress values obtained by the method proposed in this paper and shown in Table I show a dependence on anodizing current density.

Acknowledgment

The authors would like to thank J. R. de Castro for technical assistance, and they are grateful to CNPq and FAPESP for financial support.

Manuscript submitted Oct. 9, 1991; revised manuscript received Dec. 5, 1991.

Unicamp assisted in meeting the publication charges for this letter.

REFERENCES

1. J. S. L. Leach and B. R. Pearson, *Corrosion Science,* **28,** 43 (1988).
2. R. W. Hoffman, *Thin Solid Films,* **89,** 155 (1982).
3. D. A. Vermilyea, *This Journal,* **110,** 345 (1963).
4. D. M. Bradhurst and J. S. L. Leach, *ibid.,* **113,** 1245 (1966).
5. E. Klokholm, *IBM Res. Rept.,* RC 1352 (1965).
6. R. W. Hoffman, in "Thin Films," p. 99, American Society for Metals (1963).
7. S. P. Timoshenko and J. M. Gere, "Theory of Elastic Stability," 2nd Ed., McGraw Hill, Kogakusha, Tokyo (1961).